

Figure 3. Ir spectra of the quinodimethanes at 77°K (—) and polymers formed on warming to 20°C (---).

sorption bands and formation of new bands characteristic of the respective aromatic compounds. It is well known that the quinodimethanes are extremely reactive and polymerize readily, and the spectra in Figure 2 (dashed lines) are identical with those of the polymers formed by phenyllithium coupling of the corresponding di(bromomethyl) compounds.<sup>13,14</sup>

(13) J. H. Golden, *J. Chem. Soc.*, 1604 (1961).

(14) J. H. Golden, *ibid.*, 3741 (1961).

The ir spectra of the quinodimethanes at 77°K and of the polymers produced on warming to ambient temperature are shown in Figure 3. Absorption arising from the vinylidene wag in the quinodimethanes appears at 877 cm<sup>-1</sup> in **1**, 872 in **2**, and 890 in **3**.<sup>15-17</sup> Bands consistent with overtones of the wagging modes are observed at 1750, 1760, and 1790 cm<sup>-1</sup>, respectively. Further evidence for the olefinic group can be obtained from the CH stretching mode at approximately 3100 cm<sup>-1</sup>. Conjugation of the exocyclic double bond with the aromatic rings results in a diminution of the 1500-cm<sup>-1</sup> band in the quinodimethanes, whereas in the polymers where the extended conjugation is absent this band is easily detected. The band at 680 cm<sup>-1</sup> from the endocyclic double bond in **2** is analogous to the out-of-plane bending of a cis-disubstituted ethylene. This vibration is symmetry forbidden in **1** and is not observed. The bands attributed to the quinodimethanes disappear rapidly as the films are warmed to room temperature, and a new spectrum characteristic of the aromatic polymer<sup>13,14</sup> is produced.

The ir and uv spectra of the quinodimethanes **1**, **2**, and **3** clearly establish their quinonoid structure in the condensed phase at 77°K and provide direct spectroscopic evidence of the polymerization process that results on warming. The techniques used in this investigation also open the way for kinetic studies of the polymerization of quinodimethane monomers.

(15) L. J. Bellamy, "Infrared Spectra of Complex Molecules," 2nd ed, Methuen, London, 1968.

(16) L. J. Bellamy, "Advances in Infrared Group Frequencies," Methuen, London, 1968.

(17) N. B. Coltup, L. H. Daly, and S. E. Wiberly, "Introduction to Infrared and Raman Spectroscopy," Academic Press, New York, N. Y., 1964.

## An Electron Paramagnetic Resonance Study of Nitrosylmyoglobin

L. Charles Dickinson and James C. W. Chien\*

Contribution from the University of Massachusetts,  
Department of Chemistry, Amherst, Massachusetts 01002.  
Received December 5, 1970

**Abstract:** Paramagnetic resonance spectra of nitrosylmyoglobin have been obtained at 77°K for both the <sup>15</sup>NO and <sup>14</sup>NO derivatives. Principal values of the *g* tensor are  $g_{zz} = 2.0068$ ,  $g_{yy} = 1.9850$ , and  $g_{xx} = 2.0728$ . The *g* tensor is oriented such that the principal axis *x* is aligned along the crystallographic *c*\* axis and *y* and *z* are directed at 13° from the *b* and *a* axes, respectively. This result is interpreted in terms of the orientation of the NO ligand. Two hyperfine splittings are observed near the *a* axis:  $24.5 \pm 1$  G from the nitrogen in <sup>15</sup>NO ( $18.6 \pm 1$  G for <sup>14</sup>NO) and  $6.4 \pm 1$  G attributed to the  $\epsilon$  nitrogen of the 92-histidine residue (F8) are reported. The Fe-N-O bond angle appears to be 108–110°, resembling the 110° bond angle found previously in nitrosylhemoglobin.

The binding of ligands to hemoproteins has been a problem of keen and continuous interest to chemists and biochemists alike. The reasons reside with both the biological functions of these molecules and their prominent role as models for allosteric enzymes. Although X-ray crystallographic electron density maps, nuclear magnetic resonance contact shifts, Mössbauer spectra splittings, and electron paramagnetic

resonance (epr) data have contributed toward some understanding of the bonding situation, the lack of a detailed description is obvious. In particular, very little is known regarding the bonding interactions between the metal and oxygen and the relevant histidines. It is to this problem that the work of this laboratory has been directed.

The classical epr work on hemoproteins was done by

Bennett, *et al.*,<sup>1</sup> on sperm whale acid metmyoglobin (Mi) and equine acid methemoglobin (Hi). (The abbreviations used for various derivatives are: Mb, deoxymyoglobin; Mi, acid metmyoglobin; MbO<sub>2</sub>, oxymyoglobin; MiN<sub>3</sub>, metmyoglobinazide; MbNO, nitrosylmyoglobin; Hb, deoxyhemoglobin; Hi, acid methemoglobin; HbO<sub>2</sub>, oxyhemoglobin; HiN<sub>3</sub>, methemoglobinazide; HbNO, nitrosylhemoglobin.) In these cases, the paramagnetic resonances of the ferric ions have broad lines and are devoid of hyperfine splitting. Ligand bonding information is thus unavailable from these studies. Unfortunately for the epr spectroscopists, the biologically significant oxyhemoglobin and oxymyoglobin are diamagnetic.<sup>2</sup> However, each of the nitric oxide derivatives of myoglobin and hemoglobin has one unpaired electron.<sup>3</sup> Furthermore, single crystals of HbNO give epr spectra showing hyperfine splitting due to the nitrogen nucleus on NO and rhombic symmetry for both the *g* and the hyperfine tensors.<sup>4</sup> It was possible to deduce that the Fe-N-O bond angle is about 110°. However, there are extra resonance lines unaccounted for and the line widths vary in a systematic manner. Consequently, it seems worthwhile to closely examine the simpler case of MbNO single crystals to understand the origins of the extra resonance lines and of the line broadenings.

In this paper the epr data on single crystals of Mb-<sup>14</sup>N and Mb-<sup>15</sup>N are presented. For the first time, clear splittings of resonance lines due to the imidazole nitrogen of the 92 histidine (F8) have been observed, thus providing definitive proof of the frequently postulated covalent bonding between heme iron and this residue.

## Experimental Section

Epr spectra were measured on a Varian Associates E-9 spectrometer with a dual cavity. The *g* values were referenced to the *g* = 2.0036 signal of a small polycrystalline sample of DPPH in the second cavity. Spectra at liquid nitrogen temperature were made using a quartz dewar flask.

The two-circle goniometer used was a modification of a previously described model.<sup>4</sup> It was found that the myoglobin crystals froze to the Kel-F surface of the goniometer cup, thus obviating the need of any protective or securing cap for the cup. Crystals were mounted with the *ab* plane flush against the bottom of the goniometer cup. Using a low-power microscope, the cup was then rotated on its axis until the *b* axis (the long axis and the axis of maximum extinction in polarized light) was either parallel or perpendicular, as desired, to the line scored parallel to the axis of the goniometer rod. These steps were facilitated by loosely clamping the rod onto a metal block with a v-shaped groove which was fixed to the stage of the microscope. Thus the plane in which the magnetic field was rotated was accurately determined, but the zero of the angular scale of rotation could only be approximated. Previous studies such as those on metmyoglobin<sup>1</sup> could use crossing points of the signals from two inequivalent sites to very accurately determine the orientation in the chosen plane. In our data for MbNO the crossing points do not occur. Mixed crystals of Mi partially reduced with NO were used to determine the orientation within the plane, and it is on the basis of these data that the assignment of axes on the figures was confirmed. Angular rotations were measured with a 2-in. protractor attached to the goniometer rod, and spectra were recorded at intervals of at least every 10°.

Lyophilized sperm whale myoglobin crystals were supplied by Koch-Light Laboratories, Colnbrook, England. Single crystals were grown by the method of Kendrew and Parrish:<sup>5</sup> 0.2 ml of 10% Mi was added to 1.8 ml of a solution of pH 6.2 ammonium sulfate (3.5 *M*) and 0.05 *M* phosphate buffer. (The required sulfate concentration seemed to change mysteriously at times.) Crystals of the usual type-A habit<sup>6</sup> were obtained when the crystallization took place in a flat-sided cuvette; crystallizations in circular cylindrical tubes of i.d. 1 cm resulted in crystals of irregular habit.

The preparation of MbNO crystals and particularly the isotopically labeled crystals is greatly simplified by two key observations. First, like the Hi and HbNO pair,<sup>4</sup> Mi and MbNO are truly isomorphous. Secondly, Mi is also reduced by NO and converted to MiNO, though somewhat slower than the corresponding processes for hemoglobins,<sup>6</sup> and the binding of NO by Mi in MiNO is less firm by comparison.<sup>7</sup> Taking advantage of these observations, one can prepare MbNO crystals by the following simple procedure.

The Mi crystals were first flushed in their mother liquor for 1 hr with prepurified nitrogen gas (99.9+%, Airco), saturated with water vapor, and then exposed to NO at approximately 1 atm. The nitric oxide was generated by adding dilute sulfuric acid saturated with ferrous sulfate to solid sodium nitrite. The NO was then scrubbed free of the higher nitrogen oxides by using a 20-in. column of potassium hydroxide. The <sup>15</sup>N<sub>2</sub>O used was of 96.1% isotopic purity (Mallinckrodt-Nuclear) and was added by standard vacuum-line techniques. The small amount of N<sub>2</sub>O<sub>3</sub> present was kept in the solid state by a solid carbon dioxide bath.

The usefulness of mixed Mi-MbNO crystals to accurately define the crystallographic axes has already been mentioned above. Such crystals can be prepared either by incomplete reaction of the Mi crystals with NO or by permitting MbNO crystals to undergo partial autoxidation without denaturation.

The complex of NO with pyridine hemochromes was prepared by exposing a deoxygenated solution of hemin (1 mM) in pyridine to an NO atmosphere. The color change and appearance of the epr spectrum were immediate.

Because of the overlap problem, the determination of exact line positions was somewhat subjective. The apparently variant line widths and slightly irregular intensity patterns made it seem not worthwhile to simulate spectra at this stage. Several general rules were used in selecting the line positions reported in Figures 1 and 2. These rules were devised by inspection of calculated spectra patterns published by Lebedev, *et al.*<sup>8</sup> If two lines were sufficiently well resolved to exhibit two definite inflection points in the region of overlap, the field position of the half peak-to-peak point of each line on the unresolved spectrum was taken as the line position. For overlapping lines exhibiting a single inflection point, the line positions were taken as  $H_c \pm \frac{1}{4}\Delta H_{pp}$ , where  $H_c$  is the center of the overlapping pattern and  $\Delta H_{pp}$  is the apparent peak-to-peak width of the overlap patterns.

## Results

Plots of line position in gauss *vs.* angle of rotation relative to the dc magnetic field direction are given in Figure 1 for a single crystal of Mb-<sup>15</sup>N. A similar plot is given in Figure 2 for the *ab* plane of Mb-<sup>14</sup>N. The appearance of two turning points  $\pm 13^\circ$  from the *b* axis in the *ab* plane is clear evidence for two non-equivalent sites per unit cell. However, in the *bc*\* plane only one resonance was resolved. Line widths in the vicinity of *b* and *c*\* are approximately 30 G and could easily obscure sites of small *g* differences. In contrast, the line widths near *a* are only 4 G. Also, the Mb-<sup>15</sup>N spectra for the *c*\**a* plane are interpretable in the vicinity of the *a* axis as the splitting of a single line into a doublet by the <sup>15</sup>N nucleus ( $I = \frac{1}{2}$ ) with separation of  $24.5 \pm 1$  G and further splitting into triplets with separations

(1) J. E. Bennett, J. F. Gibson, and D. J. E. Ingram, *Proc. Roy. Soc., Ser. A*, **240**, 67 (1957).

(2) L. Pauling and C. D. Coryell, *Proc. Nat. Acad. Sci. U. S.*, **22**, 210 (1936).

(3) C. D. Coryell, L. Pauling, and R. W. Dodson, *J. Phys. Chem.*, **43**, 825 (1939).

(4) J. C. W. Chien, *J. Chem. Phys.*, **51**, 4220 (1969).

(5) J. C. Kendrew and R. G. Parrish, *Proc. Roy. Soc., Ser. A*, **238**, 305 (1957).

(6) J. C. W. Chien, *J. Amer. Chem. Soc.*, **91**, 2166 (1969).

(7) L. C. Dickinson and J. C. W. Chien, manuscript in preparation.

(8) Ya. S. Lebedev, D. M. Chernikova, N. N. Tikhomirova, and V. V. Voevodskii, "Atlas of Electron Spin Resonance Spectra," Consultant's Bureau, New York, N. Y., 1963.

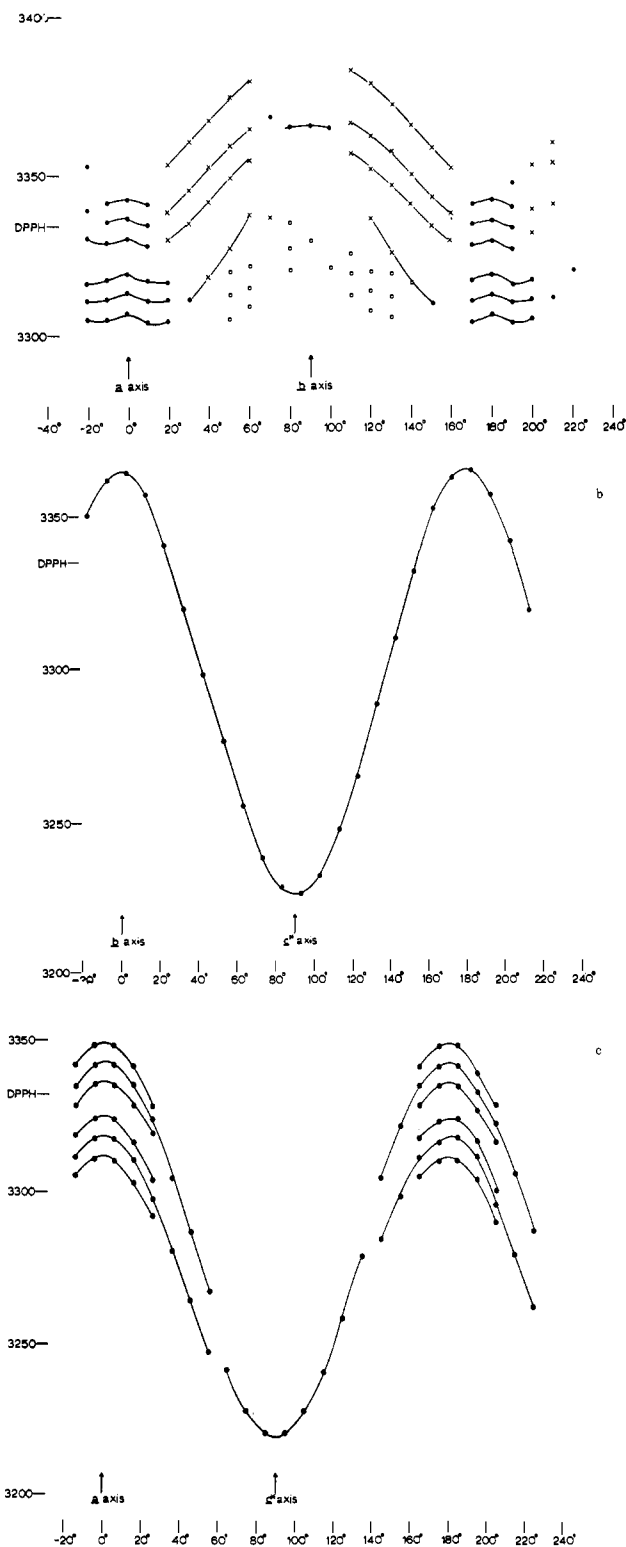


Figure 1. A plot of  $Mb^{15}NO$  resonance positions in gauss vs. angle from the  $i$  axis of the  $ij$  plane to the dc magnetic field direction at  $77^\circ K$  and  $\nu = 9.3$  GHz. Filled circles denote well-resolved lines which have accurately determined positions. Crosses denote strong lines which are severely overlapped. Squares denote a set of very weak lines. (a)  $ab$  plane, (b)  $bc^*a$  plane, (c)  $c^*a$  plane.

of  $6.4 \pm 1$  G (see Figure 3). This interpretation carries over well to the  $Mb^{14}NO$  spectra, resulting in an  $^{14}N$  ( $I = 1$ ) splitting of  $18.6 \pm 1$  G and the same triplets with a splitting of  $6.3 \pm 0.5$  G. It thus appears that a

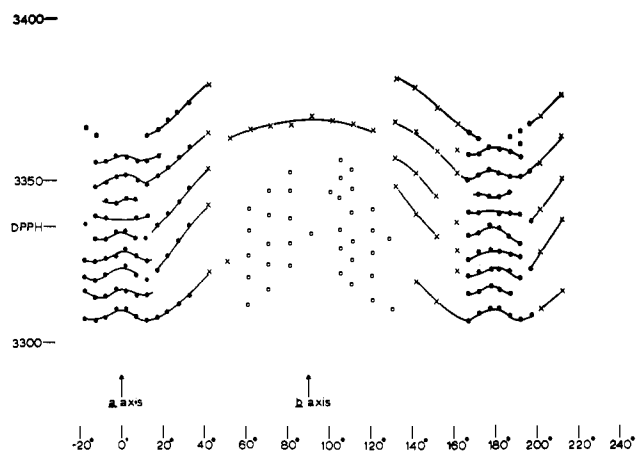


Figure 2. A plot of  $Mb^{14}NO$  resonance positions in gauss vs. angle from the  $a$  axis to the dc magnetic field at  $77^\circ K$  and  $\nu = 9.3$  GHz (see caption to Figure 1 for denotation of symbols).

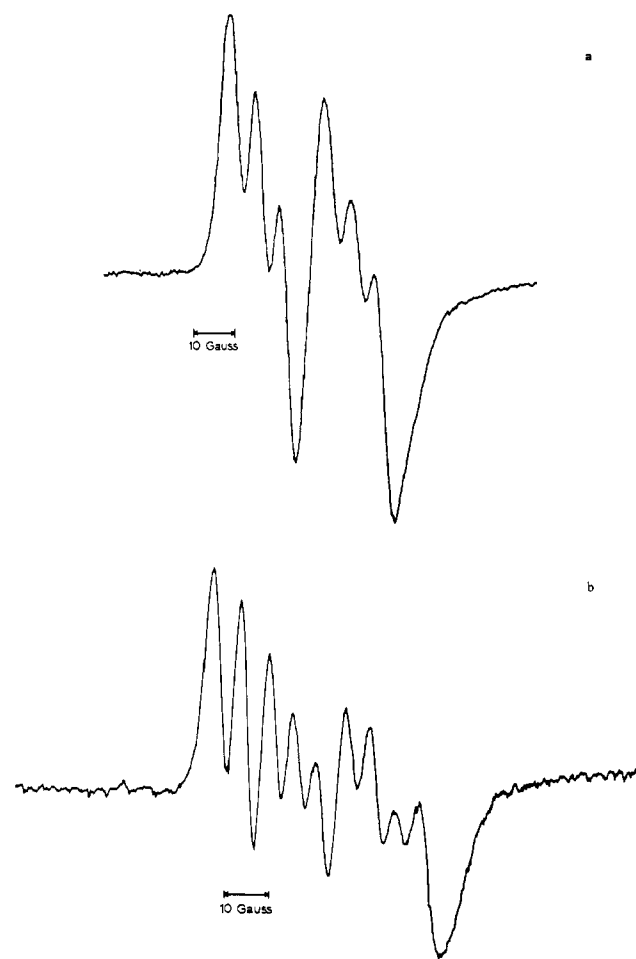


Figure 3. Epr spectra of  $MbNO$  single crystals for the dc magnetic field along the  $a$  axis of the crystal at  $77^\circ K$  and  $\nu = 9.3$  GHz. (a)  $Mb^{15}NO$ , (b)  $Mb^{14}NO$ .

single site is observed in the  $c^*a$  plane, making  $b$  a dyad axis, in agreement with X-ray results.<sup>5</sup>

Using the method of Schonland,<sup>9</sup> the principal  $g$  values for  $MbNO$  were determined. The parameters used to describe  $g$  variation with angle in the  $ij$  plane are given in Table I. Within experimental error the

(9) D. S. Schonland, *Proc. Phys. Soc.*, 73, 788 (1959).

**Table I.** Parameters Used to Describe Observed  $g$  Variation in the Crystallographic Plane  $ij$  of a Single Crystal of MbNO Using the Equation  $g_{ij}^2 = \alpha_k + \beta_k \cos 2\theta$

$ij$	$\alpha_k$	$\beta_k$
$ab$	3.981	0.045
$bc^*$	4.118	-0.179
$c^*a$	4.161	0.144

line positions were describable by the equation  $g_{ij}^2 = \alpha_k + \beta_k \cos 2\theta$ , where  $\theta$  is the angle between axis  $i$  and the direction of the dc magnetic field. The principal axes are then such that  $x$  is parallel to  $c^*$  and  $y$  and  $z$  are rotated  $+13^\circ$  from  $b$  and  $a$ , respectively (it is  $-13^\circ$  for the other site). The  $g$  values for Mb<sup>15</sup>NO and Mb<sup>14</sup>NO agree within experimental error and the average values are presented in Table II.

**Table II.** Epr Parameters for Mb<sup>15</sup>NO Single Crystals at 77°K and 9.3 GHz<sup>a</sup>

$i$	$g_i$	$A_{15N}, G$	$A_{H15}, G$
$z$	2.0068	$24.5 \pm 1$	$6.4 \pm 1$
$y$	1.9850		
$x$	2.0728		

<sup>a</sup> Orientation along the crystallographic axes of the hyperfine splittings is only approximate.

The orientation of the hyperfine tensors could not be determined with accuracy. The  $A$  tensor principal axis due to the NO nitrogen seemed to be inclined at an angle of approximately  $15\text{--}20^\circ$  away from the  $a$  axis toward the  $b$  axis and to be in the  $ab$  plane. The other splitting was not observable over a wide enough range to make any precise conclusions about the tensor orientation.

## Discussion of Results

The crystal structure of acid metmyoglobin at 1.5 Å resolution has been refined to such an extent that the locations of most of the atoms have been determined.<sup>10</sup> The heme normal makes angles of 24, 69, and  $73^\circ$  with the  $a$ ,  $b$ , and  $c^*$  axes, respectively. Almost in line with the heme normal and with a 2.2-Å internuclear distance is the  $\epsilon$  nitrogen of the F8 residue (92 His).<sup>11</sup> The iron is displaced 0.5 Å from the ring plane toward this nitrogen atom. At 4.4 Å in the opposite direction from the heme plane is the  $\epsilon$  nitrogen of the 63 His (E7). This nitrogen is considerably away from the heme normal, with the Fe-N vector making angles of 24, 68, and  $10^\circ$  with the crystallographic axes. Unfortunately, the crystal structure of MbNO has not been done.

Several theories have been forwarded for the bonding of oxygen to hemoglobin and myoglobin. As NO is quite similar in electronic structure to O<sub>2</sub> except for the subtraction of one electron, we use similar arguments for NO. Clearly, there will be differences such as that in ligand field for the two species, but at this level of interpretation we need not worry about such points. Of the several proposed structures, only two

(10) The authors are grateful to Professor J. C. Kendrew for supplying the unpublished "Myoglobin orthogonal coordinate and dihedral angle listing," April 1, 1967.

(11) For standardized labeling of residue atoms, cf. J. T. Edsall, *et al.*, *J. Biol. Chem.*, **241**, 1004 (1966).

seem to merit consideration. In structure A, the NO is bonded to the iron through one  $sp^2$  orbital pair donating into the iron  $d_{z^2}$  orbital, with contribution from bonding between the  $p\pi$  orbital of nitrogen and the  $d_{yz}$  orbital of iron. Any additional interaction between other  $sp^2$  orbitals of NO with the  $d_{zz}$  orbital of iron is probably small if at all significant. Accordingly, the Fe-N-O bond angle should be  $120^\circ$ . A second one is the  $\pi$ -bond structure (B) in which the N-O axis is perpendicular to the heme normal.

**$g$  Tensor.** The observed  $g$  tensor is rhombic with principal direction parallel to  $c$  and  $\pm 13^\circ$  from  $a$  and  $b$ . Of the three principal values, 2.0068 is assigned to  $g_{zz}$  because it is closest to the free-electron value and because it points more along the heme normal direction<sup>10</sup> than the other two components. If one assumes that the  $g$  tensors for HbNO and MbNO are not very different, then, by analogy,  $g_{zz} = 2.0728$  in MbNO. These values are, however, both smaller than the corresponding values for HbNO.<sup>4</sup> Furthermore, whereas  $g_{yy} > g_e$  in HbNO,  $g_{yy} < g_e$  in MbNO.

If  $d_{z^2}$  is the ground-state metal orbital and  $d_{zz}$  and  $d_{yz}$  are degenerate, then  $g_{yy} = g_{zz} = g_{\text{eff}} = g_e[1 - (3\lambda/\Delta)] > g_e$ , where  $\lambda$ , the spin-orbit coupling coefficient, is negative and  $\Delta \sim 10Dq$ . On the other hand, if both  $d_{z^2}$  and  $d_{yz}$  participate in the ligand binding such as for structure A, then it can be shown by second-order perturbation theory that the magnitude of  $g_{yy}$  is significantly reduced. The value of  $g_{zz}$  is not similarly affected.

The origins for the rhombic symmetry have been frequently discussed such as perturbations by the ligand, the nitrogenous residues, or some other portions of the protein. It is therefore interesting to note that solid heme apparently forms a complex with NO in the absence of any nitrogenous base. This complex has a broad epr line having  $g = 2.15$ . In the presence of pyridine, the species formed exhibits an epr spectrum in frozen solution which closely resembles that of MbNO. The  $g$  tensor has principal values of 2.11, 2.04, and 2.00. This observation indicates that nitrogenous base alone could impart a rhombic field to a metal-nitrosyl complex.

By far the most significant feature of the data is the fact that the orientations of the principal axes of the  $g$  tensor are nearly parallel to the three crystallographic axes. From the description of the heme plane and the heme normal above, if there is no major conformational change on going from Mi to MbNO, then the  $g$  tensor neither lies in the heme plane, nor does it have a principal component along the heme normal. It is recalled that none of the  $g_{zz}$  directions of the four paramagnetic centers in HbNO are parallel to the heme normals of acid Hi; the deviations observed are  $10\text{--}20^\circ$ . There are two possibilities to account for these discrepancies. One is that the heme normals in MbNO and in Mi are not the same, and they are also not the same in HbNO and in Hi. It has been noted that the heme normals for various derivatives of high-spin and low-spin methemoglobins differ by up to  $20^\circ$ .<sup>1,12,13</sup> A second possibility is that  $g_{zz}$  does not coincide with the heme normal. In the case of MiN<sub>3</sub>, the atomic posi-

(12) D. J. E. Ingram, J. F. Gibson, and M. F. Perutz, *Nature (London)*, **178**, 906 (1956).

(13) J. F. Gibson, D. J. E. Ingram, and D. Schonland, *Discuss. Faraday Soc.*, **26**, 72 (1952).

tions near the heme are presumably identical with those in Mi by three-dimensional difference Fourier transform at 2.0 Å resolution.<sup>14</sup> Nevertheless, the maximum  $g$  value in  $\text{MiN}_3$  was found<sup>15</sup> to deviate 9° from the heme normal. It is possible that both factors contribute toward the noncoincidence of  $g_{zz}$  in HbNO and MbNO with the respective heme normals in Hi and Mi. The direction of  $g_{zz}$  does not have to coincide with the heme normal if the direction cosines of the anisotropic  $g$  components are dictated by the Fe–N bond. These will point along the heme normal and heme plane if it is a simple  $\sigma$  type,  $\pi$  type, or  $sp^2$ -type bond with Fe–N–O angle of 180, 90, or 120°, respectively. For intermediate mixed bonding schemes, the  $g$  tensor will generally differ from the heme normals and heme planes.

A rigorous test of the second possibility is being carried out in this laboratory. <sup>57</sup>Fe-enriched MbNO is being prepared. Simultaneous determinations of the <sup>57</sup>Fe hyperfine tensor and of the  $g$  tensor should resolve these questions.

**Hyperfine Tensor.** Hyperfine coupling was resolved only in the vicinity of the  $a$  axis. The coupling constant is  $18.6 \pm 1$  G. This corresponds to  $T_{\eta\eta} = 19.3$  G in HbNO. From the deviation of maximum hyperfine coupling from the  $g$  value along this direction, an Fe–N–O bond angle of 108–110° is indicated for MbNO. Therefore, the same bond type is involved in both MbNO and HbNO.<sup>4</sup> In HbNO, a maximum hyperfine splitting of 27 G was observed along one of the directions perpendicular to the heme normal. This splitting was not resolved in MbNO. The line widths along this direction is inordinately broad and could well contain this hyperfine splitting (*vide infra*).

The change of the hyperfine pattern for the dc magnetic field direction near the  $a$  axis from a nine-line spectrum for <sup>14</sup>NO ( $I = 1$ ) (Figure 3a) to a six-line spectrum for <sup>15</sup>NO ( $I = 1/2$ ) (Figure 3b) implies that the resonance is split by an additional nucleus with  $I = 1$ . The  $\epsilon$  nitrogens of both the 92 His and the 63 His are possible nuclei for this interaction. The latter is believed to be protonated<sup>16</sup> in the presence of a ligand. The absence of proton hyperfine splitting favors the  $\epsilon$  nitrogen of the 92 His for the observed hyperfine splitting. This nitrogen atom is found to lie only 1.8 Å from the iron atom;<sup>10</sup> presumably, there is a transfer of spin density between them.

From the atomic positions of the F8 His given by X-ray,<sup>10</sup> the observed hyperfine splitting must be attributed to the spin polarization of the nitrogen  $sp^2$  orbital. It is unfortunate that hyperfine splitting along the  $p_z$  direction was unresolvable.

(14) L. Stryer, J. C. Kendrew, and H. C. Watson, *J. Mol. Biol.*, **8**, 96 (1964).

(15) G. A. Helcke, D. J. E. Ingram, and E. F. Slade, *Proc. Roy. Soc., Ser. B*, **169**, 275 (1968).

(16) C. D. Coryell and L. Pauling, *J. Biol. Chem.*, **132**, 769 (1940).

**Anisotropic Line Widths.** The line widths observed for MbNO are highly anisotropic. Whereas the line width is only about 4 G along the  $a$  axis, it is about 30 G in the other directions. Furthermore, the widths are significantly different for Mb<sup>15</sup>NO and Mb<sup>14</sup>NO. For example, in Figure 1b, the line widths at 10, 40, 90, and 130° are 29, 27, 26, and 25 G, respectively, for Mb<sup>15</sup>NO; they are 35, 30, 32, and 31 G for Mb<sup>14</sup>NO. Consequently, unresolved hyperfine structure must be partly responsible for the anisotropic line broadenings. However, if this were the only source of line broadening, then we expect the line widths along the  $b$  and the  $c^*$  axes to be very different. In HbNO, the hyperfine splittings along these directions are about 27 and 6 G.

There are at least two contributing factors which tend to broaden epr lines in the  $bc$  plane, which is also approximately the heme plane. One is the hyperfine splitting with the pyrrole nitrogens. Scholes<sup>17</sup> reported a value of 4.5 G for this interaction.

Another mechanism for the broad observed epr line width is the random misorientation of the symmetry axes in the crystal.<sup>15,18</sup> In the case of acid Mi and  $\text{MiN}_3$ , the large anisotropic line width can be accounted for by a  $\pm 1.5^\circ$  variation in  $\theta$ , the angle of tilt of the heme normal. In the case of  $\text{MiN}_3$  it was found that  $\phi$ , the angle of rotation of the porphyrin ring, can be as much as  $\pm 4^\circ$ . Because of the smaller  $g$  anisotropy in  $\text{MiNO}$ , the line-width contribution due to misorientation should be much smaller. One can estimate the magnitude by the following equation

$$\Delta H_{\theta, \phi=90^\circ} = \frac{h\nu (g_{zz}^2 - g_{yy}^2)}{\beta (g_{\text{eff}})^3} \sin 2\theta d\theta$$

and a similar one for  $\Delta H_{\phi, \theta=90^\circ}$ . A line-width contribution of 2.8 G is calculated for a  $\pm 1.5^\circ$  variation in  $\theta$  in 10 G for a  $\pm 4^\circ$  variation in  $\phi$ .

Some of the fine points of the epr spectra of MbNO can be resolved if greater resolution can be achieved. One type of measurement underway in this laboratory should make this possible. This is the use of electron-electron double resonance.<sup>19</sup> With this technique, the improvement in resolution achievable is the ratio of inhomogeneous line widths to this homogeneous line width. It is hoped that such study will provide more detailed understanding of the interactions between the ligand, the heme, and the relevant histidines.

**Acknowledgment.** This work was supported in part by the National Institutes of Health (Grant No. HE 14270) and by the National Science Foundation (Grant No. GB 20952).

(17) C. P. Scholes, *Proc. Nat. Acad. Sci. U. S.*, **62**, 428 (1969).

(18) P. Eisenberger and P. S. Pershan, *J. Chem. Phys.*, **47**, 3327 (1967).

(19) J. S. Hyde, J. C. W. Chien, and J. H. Freed, *ibid.*, **48**, 4211 (1968).